Defence Science Journal, Vol. 69, No. 6, November 2019, pp. 591-598, DOI : 10.14429/dsj.69.13782

Simulation of Fragmentation Characteristics of Projectile Jacket Made of Tungsten Alloy after Penetrating Metal Target Plate using SPH Method

Chun Cheng*, Zhonghua Du, Xi Chen, Lizhi Xu, Chengxin Du, and Jilong Han

School of Mechanical Engineering, Nanjing University of Science and Technology, Nanjing - 210 094, China
**E-mail: xiangchun893@163.com*

ABSTRACT

A smooth particle hydrodynamics (SPH) model was used to simulate the fragmentation process of the jacket during penetrator with lateral efficiency (PELE) penetrating the metal target plate to study the fragmentation characteristics of PELE jacket made of tungsten alloy. The validity of the SPH model was verified by experimental results. Then the SPH model was used to simulate the jacket fragmentation under different impact velocity and thickness of target plate. The influence of impact velocity and thickness of target plate on the jacket fragmentation was obtained by analysing the mass distribution and quantity distribution of the fragments formed by the jacket. The results show that the dynamic fragmentation of tungsten alloy can be simulated effectively using the SPH model, Johnson-Cook strength model, maximum tensile stress failure criterion and stochastic failure model. When the thickness of target plate is fixed, the greater the impact velocity, the greater the pressure produced by the projectile impacting the target plate; with the increase of impact velocity, the mass of residual projectile decreases, the number of fragments formed by fragmentation of jacket increases linearly, and the average mass of fragments decreases exponentially. When the impact velocity is constant, the greater the thickness of the target plate, the longer the pressure duration by the projectile impacting the target plate; with the increase of the thickness of target plate, the mass of residual projectile decreases, the number of fragments formed by fragmentation of jacket increases linearly, and the average mass of fragments decreases exponentially. The numerical calculation model and research method adopted in this paper can be used to study the impact fragmentation of solid materials effectively.

Keywords: PELE; Fragmentation; Smooth particle hydrodynamics model; Impact velocity; Thickness of target plate; Jacket fragmentation process

1. INTRODUCTION

The penetrator with lateral efficiency (PELE) is a kind of ammunition without fuze and explosive, consisting of a thick cylindrical jacket with high density and a low density filling inside. The jacket is broken to produce a large number of fragments after the projectile penetrated the metal target plate. The projectile can be used to attack high-value targets with low protective capability such as light armoured vehicle, ground parked aircraft, low-altitude hovering helicopter, command and communication equipment[1]. The fragmentation of PELE jacket is a very complicated process. The impact pressure produced by the target plate acts on the head of the jacket, and the compression and expansion of the filling results in the radial load acting on the inner wall of the jacket. The initiation, propagation and interconnection of internal cracks in the jacket under high strain rate loads eventually lead to the fragmentation of the jacket. Although the fragmentation process of PELE jacket is complex, in short, the fragmentation issue of jacket belongs to the research field of impact fragmentation of solid material. The issue of dynamic fragmentation of solid material under impact loading is a long-term research topic in the fields of elastic-plastic mechanics, dynamic mechanical properties of material, aerospace and weapon science. At present, the main methods to simulate the dynamic fracture of solid material are finite element method (FEM)[2], discrete element method (DEM)[3], finite element method combined with discrete element method[4-5], level set method[6], molecular dynamics method[7] and smooth particle hydrodynamics (SPH) method[8-10]. The finite element method is difficult to display the discontinuity accurately such as crack, for it is difficult to deal with the contact problem of the crack surface and crack propagation on multiple elements[11]. Although the finite element method with cohesive elements can reproduce explicit cracks, the disadvantage of this method is that it needs to add artificial flexibility, because even under small loads the element will inevitably open[12]. In addition, it is difficult to deal with when and where to insert cohesive elements in simulation[13]. The DEM is mostly applied to diverse problems in granular processes such as packing of particles, die filling, fragmentation of agglomerates, bulk compression, powder mixing. Though the DEM method has been applied to shock impact simulations and the fragmentation under shock compression, it is mostly applied to the fragmentation problems of brittle materials such as rock and ceramics[3]. Molecular dynamics is an effective mean to study the microcosmic world, but it is not very suitable to simulate the macroscopic fracture of materials.

During this study, SPH method is used to simulate the

Received : 16 January 2019, Revised : 24 April 2019
Accepted : 10 June 2019, Online published : 16 December 2019

dynamic fragmentation of PELE jacket. In 1995, Benz proposed SPH method for simulating solid material[14]. Because of its own characteristics, this method has great attraction in simulating the dynamic response of material such as fracture and fragmentation[15]. The SPH method is a mesh-less numerical method based on Lagrange method, which supports arbitrary large deformation and Lagrange state variable tracking, and avoids the program termination caused by grid distortion in Lagrange mesh calculation[16]. Nordendale used finite element method model and SPH model to predict the impact of high-speed projectiles on single-layer and laminated high-strength cementitious (HSC) plates[17]. The validity of the two methods was compared and verified by experiments. The results show that SPH model can simulate the formation of debris field, but FEM can not .

During the current study, SPH method was used to simulate the fragmentation process of the PELE jacket. The validity of the SPH model was verified by experimental results, then the influence of impact velocity and target thickness on jacket fragmentation was studied by the SPH model. The mass distribution and quantity distribution of the fragments formed after the fragmentation of the jacket after the PELE penetrated the metal target plate were analysed.

2. SIMULATION METHODS

The geometric model of numerical calculation is shown in Fig. 1. The projectile is composed of tungsten alloy jacket and low density material filling. The target plate is made of high strength aluminum alloy. The projectile impacts the target plate perpendicularly at a certain speed. In the process of PELE penetrating and perforating the metal target plate, the jacket undergoes plastic deformation and severe fragmentation. In order to show the process of jacket deformation and fragmentation, to count the quality and quantity of fragments formed by jacket fragmentation accurately, experimental results were used to verify the numerical simulation, then reasonable numerical model and appropriate parameters were chosen for the jacket.

During the study, SPH method was used to simulate the fragmentation process of the jacket. The distance between two adjacent particles is 0.2 mm. The Johnson-Cook strength model was used to describe the deformation and failure behaviour of tungsten alloy jacket in the process of PELE penetrating target plate. Rohr studied the relationship between yield stress and strain rate of tungsten alloy material in 10 strain rate scales (5×10^{-5} ~2.7×10^{-5} s-1) by tensile test, modified Taylor impact test and plate impact test. The parameters of Johnson-Cook strength model and state equation for describing dynamic deformation and failure of tungsten alloy materials were obtained. The Johnson-Cook strength model was validated by modified Taylor impact test and numerical simulation. It is proved that the Johnson-Cook strength model can effectively simulate the dynamic deformation and failure behaviour of tungsten alloy materials[18].

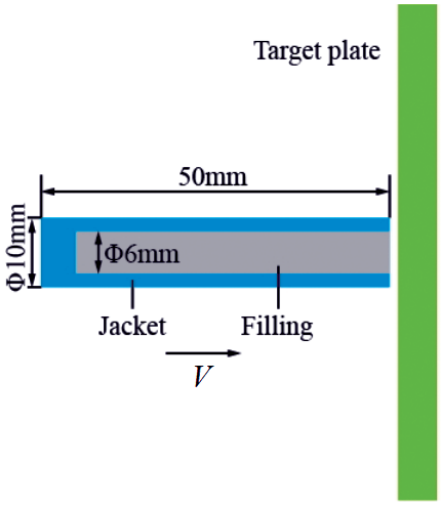

Figure 1. Geometric model diagram of numerical calculation.

The target plate is made of aluminium alloy, and fixed boundary constraints are set around the target plate. The target plate is seriously plastic deformed and destroyed under the impact of projectile. Therefore, the Johnson-Cook model is also used for the material of the target plate (aluminum alloy). In order to truly reflect the plugging phenomenon of the target plate, the geometric erosion failure strain was set to 1 for the target plate model in the simulation. The main parameters of the material are as shown in Table 1[19-20].

Table 1. Main parameters of Johnson-Cook strength model for tungsten alloy and aluminum alloy

	Tungsten alloy	Aluminum alloy
Density (g/cm$^{3)}$	18	2.77
Poisson's ratio	0.3	0.33
Modulus of elasticity (GPa)	360	71.7
Yield stress (MPa)	1350	497
Hardening constant (MPa)	177	310
Thermal softening coefficient	1	1.426
Hardening exponent	0.12	0.185
Melting temperature (K)	1723	863
Reference strain (rate/s^{-1})	1	1
Specific heat capacity J(kgK)$^{-1}$	134	921

Based on the brittle fracture behaviour of tungsten alloy, especially high density tungsten alloy under dynamic loading, the tensile principal stress failure criterion describing the failure of brittle materials was added to the Johnson-Cook strength model in the fracture simulation of PELE jacket. The fragments have obvious statistical characteristics of probability, because the fragments are random when the jacket is broken, but the structure and material of the jacket are uniform and the material properties are unique in numerical simulation. Therefore, in order to simulate the random characteristics of the jacket fragmentation, the stochastic failure model based on Mott's theory was introduced to the failure criterion of tensile principal stress in numerical simulation. In this model, Mott simplifies a cylindrical shell into a two-dimensional ring according to its radial cross-section, and assumes that the probability of fracture occurring on an unbroken shell of unit length along the circumferential direction when the strain changes from ε to $\varepsilon + d\varepsilon$[21].

$$dp = D\exp(\gamma\varepsilon)d\varepsilon \quad (1)$$

where p is the probability of fracture. D and γ are material characteristic parameters respectively, which related to loading strain rate. The probability of fracture increases exponentially with strain increasing. It is assumed that when the strain is ε, the probability of unbroken of the shell is 1-p, in that way, when the strain increases by $d\varepsilon$, the probability that the shell will fracture is as follows,

$$dp = (1-p)D\exp(\gamma\varepsilon)d\varepsilon \quad (2)$$

After solving the integral, it is possible to get the probability p of fracture before a certain point of the shell reaches plastic strain.

$$p = 1-\exp\left[-\frac{D}{\gamma}\exp(\gamma\varepsilon)\right] \quad (3)$$

Mott considers that the average fracture strain $\overline{\varepsilon}$ exists in the material.

$$\overline{\varepsilon} = \frac{1}{\gamma}\left[ln\left(\frac{\gamma}{D}\right)-05772\right] \quad (4)$$

The standard deviation of the average fracture strain is as follows:

$$\sigma_\varepsilon = \left[\int_0^\infty (\varepsilon-\overline{\varepsilon})^2\, dp\right]^{1/2} = \frac{1}{\gamma}\frac{\pi}{\sqrt{6}} \approx \frac{1.282}{\gamma} \quad (5)$$

3. DISCUSSION

3.1 Numerical Result and Validation

To verify the rationality of numerical model and parameter selection, the experiment[1] was numerically calculated, and the numerical results were compared with the experimental results. The jacket is made of tungsten alloy, the diameter and length are 10 mm, 50 mm respectively. The filling is made of low density aluminum alloy, the diameter and length are 6 mm, 45mm respectively. The target plate is made of aluminum alloy with a thickness of 8 mm. The impact velocity is 1254 m/s. The numerical result and the fragmentation of the projectile after penetrated the target plate taken by X-ray in the experiment are as shown in Fig. 2. The numerical result is very similar to the experimental picture. The experimental results show that the residual projectile velocity is 1208 m/s, the maximum radial velocity of fragments is 221 m/s, while the residual projectile velocity is 1216.39 m/s, and the maximum radial velocity of fragments is 220.38 m/s using numerical model. The errors are 0.69 per cent and 0.28 per cent, respectively. The numerical results are in good agreement with the experimental results, which fully demonstrates the rationality of the numerical model and parameters selection.

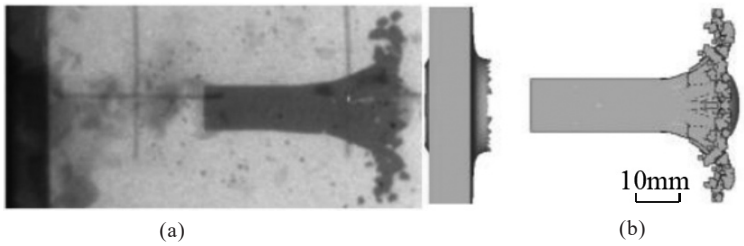

Figure 2. Experimental and numerical result (a) experimental result and (b) numerical result.

3.2 Influencing Factors of Jacket Fragmentation

3.2.1 Impact Velocity

When the PELE jacket was made of tungsten alloy, 10mm in diameter and 50 mm in length, the filling was made of nylon, with a diameter of 6 mm and a length of 45 mm, the target plate was made of aluminum alloy, 5 mm in thickness, the impact velocity of the projectiles were 800 m/s, 1000 m/s, 1500 m/s, 2000 m/s, 2500 m/s respectively, the fragmentation of the projectiles at 200 mm behind the target plates was as shown in Fig. 3. As can be seen from Fig. 3,

(i) The higher the impact velocity, the smaller the volume of the residual projectile, which means the smaller the mass of the residual projectile. The statistical mass of the residual projectile m_r is as shown in Fig. 4(a).

(ii) When the impact velocity is low, the projectile jacket breaks into larger fragments, and the shape of fragments is regular long strip. As the impact velocity increases, the shape of the fragments becomes more irregular and the smaller the volume is.

(iii) The number of fragments formed by PELE jacket fragmentation increases with the increase of impact velocity.

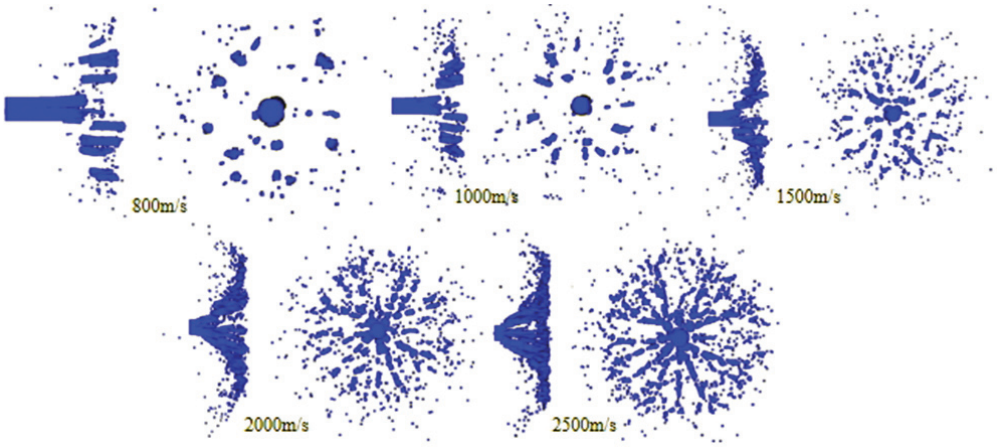

Figure 3. Fragmentation of PELE jacket at 200 mm behind the target plates under different velocities.

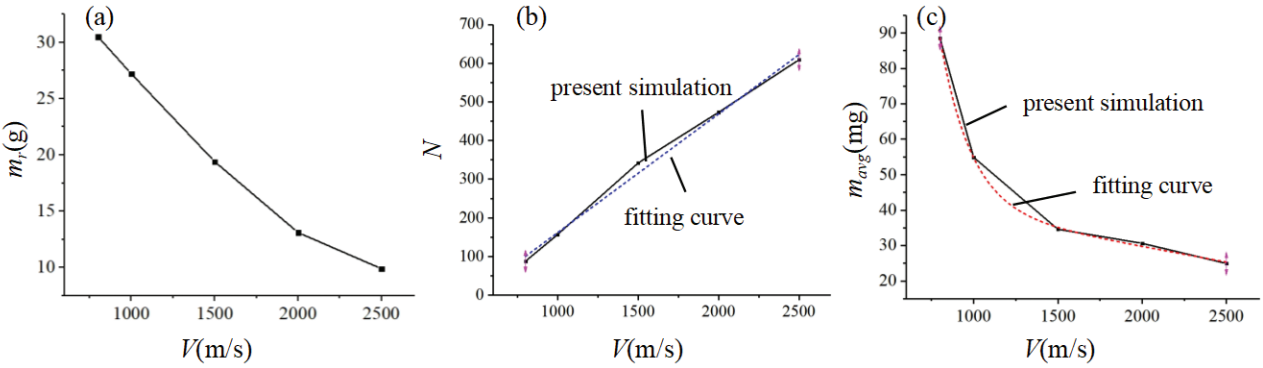

Figure 4. Mass of the residual projectile m_r, number of fragments N and average mass of the fragments m_{avg} changes with the impact velocity V.

The number of fragments N produced by the fragmentation of the projectile jacket changes with the impact velocity V was calculated, as shown in Fig. 4(b). The number of fragments increases almost linearly with the increase of impact velocity.

When the projectile impacts the target plate at a certain velocity of V, the pressure in the filling is P_f , as follows[22].

$$P_f = \rho_f C_f \left(V - U_t\right) + \rho_t S_f \left(V - U_t\right)^2 \quad (6)$$

where ρ_f and ρ_t denote the density of filling and target plate, respectively. V is the impact velocity. C_f represents the sound velocity in filling. S_f and U_t denote parameter in equation of state of filling material and velocity of particles after wave front of target plate, respectively.

It can be seen from the Eqn. (8) that the pressure in the filling increases with the increase of impact velocity, therefore the axial stress σ_{axial} in the loading increases with the increase of impact velocity. According to the generalised Hooker's law, the radial stress σ_{axial} is as follows[23].

$$\sigma_{radial} = \mu\sigma_{axial} \quad (7)$$

where μ is Poisson's ratio. It can be concluded that the force produced by the filling acting on the inner wall of the jacket increases with the increase of impact velocity, and the radial acceleration and strain rate of the jacket increase. According to the law of impact fragmentation of solid material[24], with the increase of impact strain rate, the more fragments produced by material fragmentation, the smaller the average mass of fragments. Therefore, with the increase of impact velocity, the number of fragments formed by PELE jacket fragmentation increases, and the average mass of fragments m_{avg} decreases. The average mass of the fragments m_{avg} varies with the impact velocity V is shown in Fig. 4(c). The average mass of fragments m_{avg} decreases exponentially with the increase of impact velocity V.

To further study the quality and quantity distribution of fragments, the cumulative quantity function of fragments $N(m)$ is defined as follows.

$$N(m) = \sum N_{fragment}(M \geq m) \qquad (m > 0) \quad (8)$$

The function $N(m)$ indicates that the cumulative number of the fragments whose mass M is greater than or equal to m. In like manner, the cumulative mass function of fragments $M(m)$ is defined as follows.

$$M(m) = \sum M_{fragment}(M \geq m) \qquad (m > 0) \quad (9)$$

The function $N(m)$ indicates that the cumulative mass of the fragments whose mass M is greater than or equal to m. According to the numerical results, the fragments mass was divided into five orders of magnitude (10e-4g, 10e-3g, 10e-2g, 10e-1g, 10e-0g), and the number of fragments in each order of magnitude was counted. The cumulative number function curve $N(m)$ and cumulative mass function curve $M(m)$ of fragments under different impact velocities V are plotting as shown in Fig. 5.

As can be seen from Fig. 5, when the impact velocity increases from 800 m/s to 2500 m/s, the number of fragments with mass order of 10e-0g is basically the same, and the

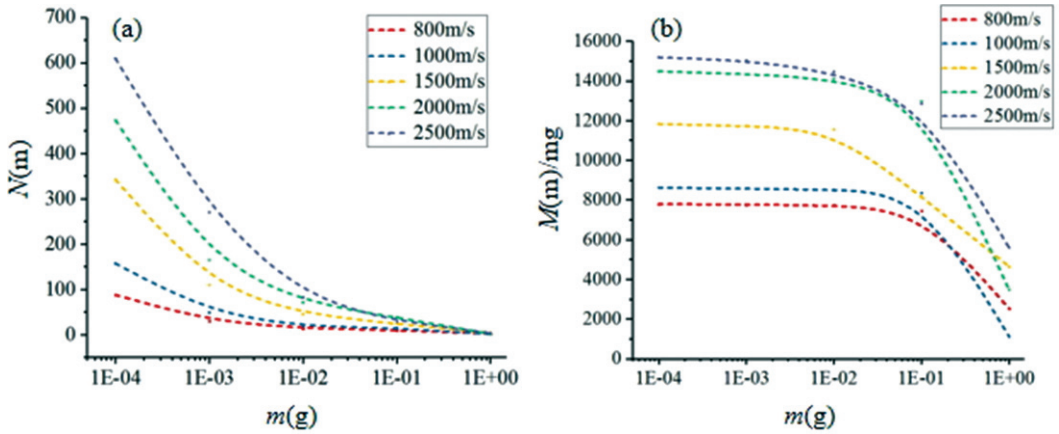

Figure 5. Cumulative number function curve $N(m)$ and cumulative mass function curve $M(m)$ of fragments under different impact velocities V.

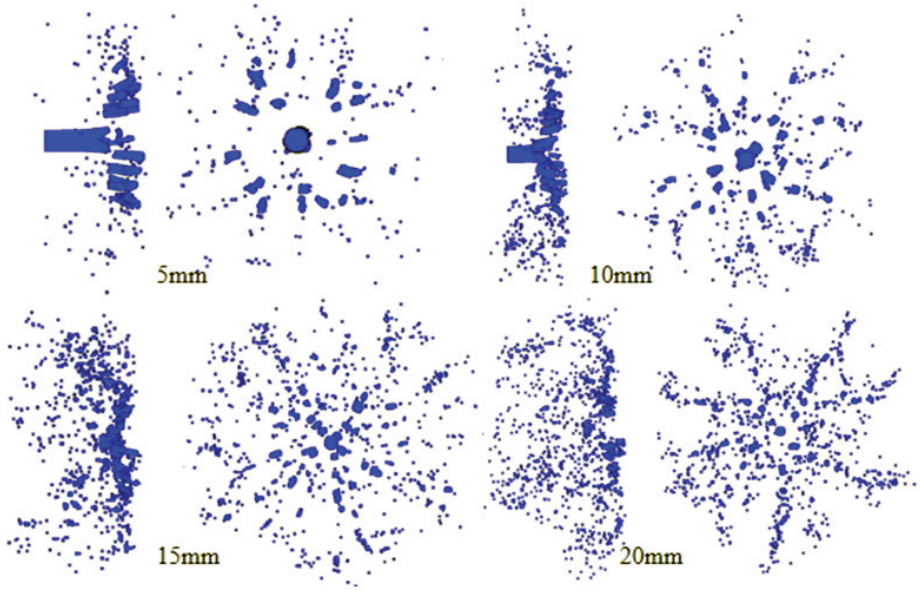

Figure 6. Fragmentation of projectiles at 200 mm behind the target plates under different thickness of target plates.

number of fragments with other mass orders increases with the impact velocity increasing. From the curves, it is can be seen that when the impact velocities are 800 m/s and 1000 m/s, the change trend of the cumulative quantity curve of fragments is relatively gentle. When the impact velocities are 1500 m/s, 2000 m/s, and 2500 m/s, the cumulative quantity curve of fragments shows a sharp downward trend. Which indicates that the amount of fragments on different mass orders is relative uniform when the impact velocities are 800 m/s and 1000 m/s, and the amount of fragments on different mass orders is uneven when the impact velocities are 1500 m/s, 2000 m/s, and 2500 m/s. The number of fragments on the 10e-4g mass order level is the largest, followed by fragments on the 10e-3g, 10e-2g mass order level, the proportion of fragments in the 10e-1g and 10e-0g mass order class to the total number of fragments is very small. When the impact velocities are 800 m/s to 2500 m/s, the accumulative mass of fragments changes smoothly when the mass of fragment is less than 10e-1g mass order. When the mass of fragment is more than 10e-1g mass order, the accumulative mass of fragments decreases sharply. This indicates that the mass of fragments with the mass of or more than 10e-1g mass order accounts for the vast majority of total fragments mass.

3.2.2 Thickness of Target Plate

When the PELE jacket was made of tungsten alloy, 20 mm in diameter and 50 mm in length, the filling was made of nylon, with a diameter of 6 mm and a length of 45 mm, the impact velocity of the projectiles was 1000 m/s, the target plate was made of aluminum alloy, the thickness of target plates were 5 mm, 10 mm, 15 mm and 20 mm respectively, the fragmentation of the projectiles at 200 mm behind the target plates was as shown in Fig. 6.

(i) The larger the target plate thickness is, the smaller the volume of the residual projectile, which means the smaller the mass of the residual projectile. The statistical mass of the residual projectile m_r is as shown in Fig. 7(a).

(ii) When the target plate thickness is small, the projectile jacket breaks into larger fragments, and the shape of fragments is regular long strip. As the thickness of target plate increases, the shape of the fragments becomes more irregular and the smaller the volume is.

(iii) The number of fragments formed by projectile jacket fragmentation increases with the increase of target plate thickness. The number of fragments produced by the fragmentation of the projectile jacket changes with the

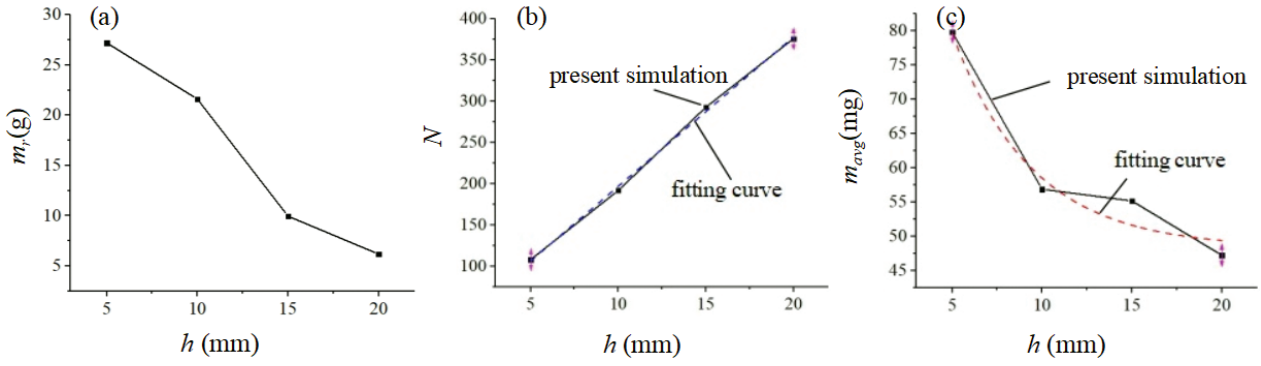

Figure 7. Mass of the residual projectile m_r, number of fragments N and average mass of the fragments m_{avg} changes with target plate thickness h.

thickness of target plate h was calculated, as shown in Fig. 7(b). The number of fragments increases almost linearly with the increase of target plate thickness.

In the process of projectile impacting and penetrating target plate, the projectile jacket plays an important role because of its high density and strength. Assuming that the plug has the same velocity as the projectile when the target plug is formed and the compression of the plug to the filling ends, the penetration time of the projectile jacket to the target plate equals the pressure action time of the target plate to the filling. When the projectile impacts the target plate, the velocity of the contact surface between the jacket and the target plate is V_I, as follows[1].

$$V_I = V\frac{\rho_j U_j}{\rho_j U_j + \rho_t U_t} \tag{10}$$

where ρ_j, ρ_t denote the density of jacket and target plate respectively. V is the impact velocity. U_j, U_t denote velocity of particles after wave front of jacket and target plate respectively.

The penetration time t is as follows.

$$t = h_I / V_I \tag{11}$$

where h_I denotes the notional distance of the contact surface between the jacket and the target plate.

Assuming that the thickness of target plate is h, the sound velocity in the target plate c_t can be expressed in lower form.

$$c_t = \frac{h + (h - h_I)}{t} \tag{12}$$

The pressure duration t can be obtained as follows:

$$t = \frac{2h}{c_t + V_I} = \frac{2h}{c_t + V\dfrac{\rho_j U_j}{\rho_j U_j + \rho_t U_t}} \tag{13}$$

When the impact velocity is constant, the duration of pressure is proportional to the thickness of target plate. In a certain thickness range, with the increase of the thickness of target plate, the more work the pressure of the target plate does on the filling, the more energy the filling provides for the shell fragmentation, the smaller the mass of the residual projectile, the more fragments the projectile jacket produces, and the smaller the average mass of the fragments. The average mass of the fragments m_{avg} varies with the thickness of target plate h is as shown in Fig. 7(c). The average mass m_{avg} of fragments decreases almost exponentially with the increase of the thickness of target plate h.

In like manner, the cumulative quantity function of fragments $N(m)$ is defined as follows.

$$N(m) = \sum N_{fragment}(M \geq m) \qquad (m > 0) \tag{14}$$

The function $N(m)$ indicates that the cumulative number of the fragments whose mass M is greater than or equal to m. Meanwhile, the cumulative mass function of fragments $M(m)$ is defined as follows.

$$M(m) = \sum M_{fragment}(M \geq m) \qquad (m > 0) \tag{15}$$

The function $N(m)$ indicates that the cumulative mass of the fragments whose mass M is greater than or equal to m. According to the numerical results, the fragments mass was divided into five orders of magnitude (10e-4g, 10e-3g, 10e-2g, 10e-1g, 10e+0g), and the number of fragments in each order of magnitude was counted. The cumulative number function curve $N(m)$ and cumulative mass function curve $M(m)$ of fragments under different thickness of the target plate h are plotting as shown in Fig. 8 . As can be seen from Fig. 8, with the increase of the thickness of target plate, the number of fragments formed by the shell fragmentation increases gradually, and the total mass of the fragments increases gradually. When the thickness of target plate increases from 5 mm to 20 mm, the number of fragments with mass equal to or greater than 10e-1g mass order is not much different, and the proportion of this part of fragments to the total quantity is small, but the mass of this part of fragments accounts for a larger proportion of the total mass of fragments, so a sharp decease trend of $M(m)$ can be as seen in Fig. 8(b).

4. CONCLUSIONS

During the study, smooth particle hydrodynamics (SPH) method was used to simulate the fragmentation process of the jacket. The validity of the SPH model was verified by experimental results. The SPH model was used to simulate the jacket fragmentation under different impact velocity and thickness of target plate. The influence of impact velocity and target thickness on the jacket fragmentation was obtained by analyzing the mass distribution and quantity distribution of the fragments formed by the jacket. Several conclusions could be drawn from the results described above.

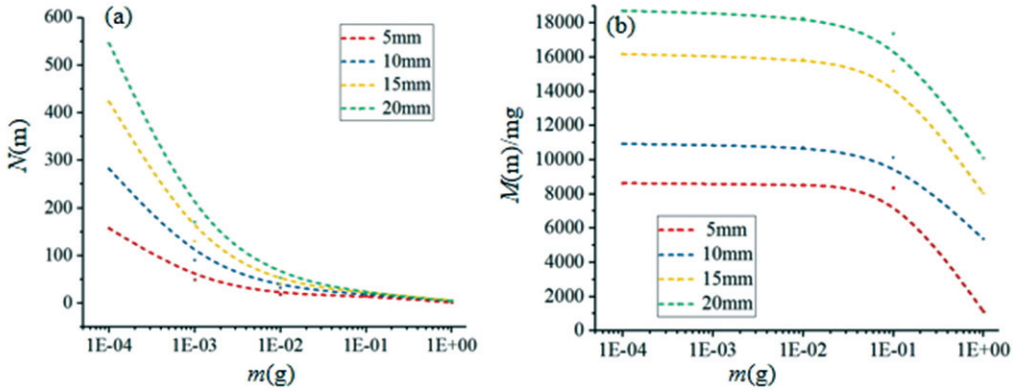

Figure 8. Cumulative number function curve $N(m)$ and umulative mass function curve $M(m)$ of fragments under different thickness of the target plate h.

The dynamic fracture of tungsten alloy can be simulated effectively using SPH method, Johnson-Cook strength model, maximum tensile stress failure criterion and stochastic failure model. The impact velocity of projectile and the thickness of target plate have a similar effect on the fragmentation of PELE jacket. When the thickness of target plate is fixed, with the increase of impact velocity the mass of PELE residual projectile decreases, the number of fragments formed by fragmentation of jacket increases linearly, and the average mass of fragments decreases exponentially. When the impact velocity is constant, with the increase of the thickness of target plate, the mass of PELE residual projectile decreases, the number of fragments formed by fragmentation of jacket increases linearly, and the average mass of fragments decreases exponentially. The fragments formed after PELE penetrating the metal target plate having a mass equal to or exceeding 10e-1g mass order accounts for the vast majority of the mass of total fragments, but the number of these fragments accounts for a very small proportion of the quantity of total fragments. The issue of dynamic fragmentation of solid material under impact loading is a long-term research topic in the fields of elastic-plastic mechanics, dynamic mechanical properties of material, aerospace and weapon science. The numerical calculation model and research method adopted in this paper can be used to study the impact fragmentation of solid materials effectively.

REFERENCES

1. Paulus, G. & Schirm, V. Impact behaviour of PELE projectiles perforating thin target plates. *Int. J. Impact Eng*., 2006, **33**(1–12), 566-579. doi: 10.1016/j.ijimpeng.2006.09.026
2. Nguyen, V.P. Discontinuous Galerkin/extrinsic cohesive zone modeling: Implementation caveats and applications in computational fracture mechanics. *Eng. Fract. Mech.*, 2014, **128**, 37-68. doi: 10.1016/j.engfracmech.2014.07.003
3. Watson, E. & Steinhauser, M.O. Discrete particle method for simulating hypervelocity impact phenomena. *Materials*, 2017, **10**(4), 379. doi: 10.3390/ma10040379
4. An, H.M; Liu, H.Y.; Han, H.; xin, Z. & Wang, X.G. Hybrid finite-discrete element modelling of dynamic fracture and resultant fragment casting and muck-piling by rock blast. *Comput. Geotech*., 2017, **81**, 322-345. d oi: 10.1016/j.compgeo.2016.09.007
5. Paluszny,A.; Tang, X.H.; Nejati, M. & Zimmerman, R.W. A direct fragmentation method with Weibull function distribution of sizes based on finite-and discrete element simulations. *Int. J. Solids Struct*., 2016, **80**, 38-51. doi: 10.1016/j.ijsolstr.2015.10.019
6. Stershic, A.J.; Dolbow, J.E. & Moes, N. The thick level-set model for dynamic fragmentation. *Eng. Fract. Mech.*, 2017, 172, 39-60. doi: 10.1016/j.engfracmech.2016.12.012
7. Sreten, M. Phenomenology of the maximum fragment mass dependence upon ballistic impact parameters. *Lat. Am. J. Solids Tru*., 2017, **14**(8), 1529-1546. doi: 10.1590/1679-78253058
8. Chakraborty, S.; Islam, M.R.I.; Shaw, A.; Ramachandra, L. & Reid, S.R. A computational framework for modelling impact induced damage in ceramic and ceramic-metal composite structures. *Compos. Struct*., 2016, 164, 263-276. doi: 10.1016/j.compstruct.2016.12.064
9. Ito, S.I. & Yukawa, S. Dynamical scaling of fragment distribution in drying paste. *Phys. Rev. E*, 2014, **90**(4), 042909. doi: 10.1103/PhysRevE.90.042909
10. Chakraborty, S. & Shaw, A. Prognosis for ballistic sensitivity of pre-notch in metallic beam through mesh-less computation reflecting material damage. *Int. J. Solids Struct.*, 2015, 67-68, 192-204. doi:10.1016/j.ijsolstr.2015.04.021
11. Vocialta, M.; Richart, N. & Molinari, J. 3D dynamic fragmentation with parallel dynamic insertion of cohesive elements. *Int. J. Numer. Meth. Eng.*, 2017, **109**(12),1655-1678 doi: 10.1002/nme.5339
12. Falk, M.L.; Needleman, A. & Rice, J.R. A critical evaluation of cohesive zone models of dynamic fracture. *Le Journal De Physique IV*, 2001, **11**(PR5), 43-50. doi: 10.1115/1.4023110
13. Camacho, G.T. & Ortiz, M. Computational modelling of impact damage in brittle materials. *Int. J. Solids Struct.*, 1996, **33**(20-22), 2899-2938. doi: 10.1016/0020-7683(95)00255-3
14. Benz, W. & Asphaug, E. Simulations of brittle solids using smooth particle hydrodynamics. *Comp. Phys. Commun.*, 1995, **87**(1), 253-265. doi: 10.1016/0010-4655(94)00176-3
15. Randles, P.W. & Libersky, L.D. Smoothed Particle Hydrodynamics: Some recent improvements and applications. *Comp. Method. Appl. M.*, 1996, **139**(1-4), 375-408. doi: 10.1016/S0045-7825(96)01090-0
16. Moxnes, J. & Steinar, B. Simulation of natural fragmentation of rings cut from warheads. *Defence Technology*, 2015, **11**(4), 319-329. doi: 10.1016/j.dt.2015.05.005
17. Nordendale, N.A.; Heard, W.F.; Sherburn, J.A. & Basu, P. A comparison of finite element analysis to smooth particle hydrodynamics for application to projectile impact on cementitious material. *Comp. Part. Mech.*, 2016, **3**(1), 53-68. doi: 10.1007/s40571-015-0092-1
18. Rohr, I.; Nahme, H.; Thoma, K. & Anderson Jr, C.E. Material characterisation and constitutive modelling of a tungsten-sintered alloy for a wide range of strain rates. *Int. J. Impact Eng.*, 2008, **35**(8), 811-819. doi: 10.1016/j.ijimpeng.2007.12.006
19. Verreault, J. Analytical and numerical description of the PELE fragmentation upon impact with thin target plates. *Int. J. Impact Eng.*, 2015, **76**(76), 196-206. doi: 10.1016/j.ijimpeng.2014.09.012
20. Rongmei, L.; Dewu, H.; Mingchuan, Y.; Enling, T.; Meng, W. & Liping, H. Penetrating performance and "self-

sharpening" behavior of fine-grained tungsten heavy alloy rod penetrators. *Mat. Sci. A-Struct.*, 2016, 675, 262-270. doi: 10.1016/j.msea.2016.08.060

21. Mott, N.F. Fragmentation of shell cases. *Proce. Royal Soc. London. Series A, Math. Phys. Sci.*, 1947, **189**(1018), 300-308. doi: 10.2307/97828
22. Meyers, M.A. & Marr, L.E . Shock waves and high-strain-rate phenomena in metals. *J. Appl. Mech.,* 1982, **49**(3), 398-399. doi: 10.1115/1.3162565
23. Chakraborty, S.; Shaw, A.; & Banerjee, B. An axisymmetric model for Taylor impact test and estimation of metal plasticity. *Proce. Royal Soc. London.* 2015, **471**(2174). doi: 10.1098/rspa.2014.0556
24. Ramesh, K.T.; Hogan, J.D.; Kimberley, J. & Stickle, A. A review of mechanisms and models for dynamic failure, strength, and fragmentation. *Planet. Space Sci.*, 2015, **107**, 10-23. doi: 10.1016/j.pss.2014.11.010

ACKNOWLEDGMENTS

The work was supported by National Natural Science Foundation of China (Grant No. 11802141) and Postgraduate Research & Practice Innovation Program of Jiangsu Province (Grant No. KYCX18_0465).

CONTRIBUTORS

Mr Chun Cheng is presently pursuing his PhD in armament science and technology from Nanjing university of Science and Technology. His current area of research includes light protective armor, experiment and simulation of terminal trajectory, fragmentation of solid material.
His contribution in the current study includes approach, theoretical analysis towards the numerical results and paper writing.

Dr (Mrs) Xi Chen obtained her PhD from the Nanjing university of Science and Technology in 2014. Currently working as an Assistant Professor of Nanjing University of Science and Technology. Her current area of research interests include damage and protection technology, impact dynamics and material mechanics properties.
Her contribution in the current study is data processing.

Dr Zhonghua Du obtained his PhD (Ammunition Engineering) from the Nanjing University of Science and Technology, in 2002. Currently, working as a Professor at the Nanjing university of Science and Technology. His main areas of research include terminal damage of projectile impacting on different target plates, such as metal plate, carbon fiber laminate panels, ceramic plate and concrete slab, development of high explosive anti-tank cartridge with high efficiency of damage, active protection system applied to infantry fighting vehicle and self-propelled artillery.
His contribution in the current study is overall guidance during the work.

Mr Lizhi Xu is presently pursuing his PhD in armament science and technology from Nanjing University of Science and Technology. He mainly studies the dynamic mechanical properties of polymer materials, the compression expansion properties of polymer materials and the impact compression properties of materials.
In the current study, he has done mechanical property analysis of tungsten alloys.

Mr Chengxin Du is presently pursuing his PhD in armament science and technology from Nanjing University of Science and Technology. He has designed and developed some new types armor piercing projectile based using tungsten alloy or Zirconium based amorphous composites.
In the current study, he has done numerical simulation design.

Mr Jilong Han is presently pursuing his PhD in armament science and technology from Nanjing University of Science and Technology. His current research interests are mechanical properties of amorphous material, experiment and simulation of high explosive anti-tank cartridge.
In the current study, he has done experimental data processing.